Atmospheric Environment 109 (2015) 31–41

Contents lists available at ScienceDirect

Atmospheric Environment

journal homepage: www.elsevier.com/locate/atmosenv

Seasonal variation of organochlorine pesticides in the gaseous phase and aerosols over the East China Sea

Tianyi Ji [a], Tian Lin [b, *], Fengwen Wang [a], Yuanyuan Li [a], Zhigang Guo [a, *]

[a] Shanghai Key Laboratory of Atmospheric Particle Pollution Prevention, Center for Atmospheric Chemistry Study, Department of Environmental Science and Engineering, Fudan University, Shanghai 200433, China
[b] State Key Laboratory of Environmental Geochemistry, Institute of Geochemistry, Chinese Academy of Sciences, Guiyang 550002, China

HIGHLIGHTS

- 80 paired gaseous phase and PM2.5 samples were collected for OCP analysis in the ECS.
- Higher particulate OCPs were observed in winter due to the continental outflow.
- The inconsistent pattern of the individual OCPs in the gaseous phase was observed.
- There was a short-term application of DDTs and Chlordanes in the upwind areas.

ARTICLE INFO

Article history:
Received 2 November 2014
Received in revised form
27 February 2015
Accepted 4 March 2015
Available online 6 March 2015

Keywords:
OCP
Gaseous phase
Aerosols
Seasonal variation
Source
East China Sea

ABSTRACT

Eighty paired gaseous phase and PM2.5 (particulate matter < 2.5 μm in diameter) samples, covering four seasons from October 2011 to August 2012 were collected simultaneously from a remote island in the East China Sea (ECS). The samples were analyzed for organochlorine pesticides (OCPs) to determine their seasonal variation and potential sources over the coastal marine environment. The concentrations of individual OCPs in the PM2.5 samples were higher in winter and lower in summer, and the reverse trend was observed for the measured OCP compounds (except hexachlorocyclohexanes, HCHs) in the gaseous phase. Principal component analysis revealed one trend that contributed 40% to PM2.5-bound OCPs characterized by β-HCH, α-HCH, *p,p′*-dichlorodiphenyldichloroethane (*p,p′*-DDD), *p,p′*-dichlorodiphenyldichloroethylene (*p,p′*-DDE), and chlordanes; whereas two seasonal trends, represented by dichlorodiphenyltrichloroethanes (DDTs) or chlordanes and HCHs, were responsible for 38% and 23% of the gaseous OCPs, respectively. Continental outflow driven by the East Asian monsoon brought large quantities of particulate OCPs to the ECS, especially in winter. Possible fresh sources or net volatilization from the Yangtze River induced by both higher ambient temperature and higher discharge rates caused the higher gaseous DDT and chlordane levels observed in summer. However, the lower concentrations of gaseous HCHs observed in summer suggested that net volatilization had a relatively limited impact on gaseous HCHs due to the long-term prohibition of their use and their low residual levels in the catchment, whereas the elevated concentrations of gaseous HCHs in winter controlled by gas–particle partitioning, resulted from increased particulate HCHs producing a partial shift to gaseous HCHs over ECS.
© 2015 Elsevier Ltd. All rights reserved.

1. Introduction

Organochlorine pesticides (OCPs), a group of persistent organic pollutants (POPs), are ubiquitous in the environment, and have been a subject of concern for several decades due to their environmental persistence, bioaccumulation, and adverse effects on living organisms (Aigner et al., 1998; Kallenborn et al., 1998; Jones and de Voogt, 1999). Due to their environmental persistence and semi-volatility in the atmosphere, OCPs are subject to long-range transport or "the Grasshopper Effect" after emission from their original source regions, resulting in global-scale distribution and pollution (Wania and Mackay, 1995; Wania et al., 1999). OCPs have been widely detected even in Antarctica (Dickhut et al., 2005; Galbán-Malagón et al., 2013a) and the Arctic (Becker et al., 2012). OCP concentrations in the atmosphere are decreasing significantly

* Corresponding authors.
E-mail addresses: lintian@vip.gyig.ac.cn (T. Lin), guozgg@fudan.edu.cn (Z. Guo).

http://dx.doi.org/10.1016/j.atmosenv.2015.03.004
1352-2310/© 2015 Elsevier Ltd. All rights reserved.

due to the global prohibition of their use (Iwata et al., 1993; Li, 1999; Weber et al., 2010). Under this regime of declining primary sources, secondary sources are becoming increasingly influential (Nizzetto et al., 2010; Gioia et al., 2012). When OCPs are used, direct supply can contribute to elevated OCP concentrations in both the ambient and remote atmosphere due to their atmospheric transport. In contrast, soils are considered to be important sinks of OCPs, as well as potential secondary sources. The sources of emission from soils to the atmosphere include direct volatilization from soils and transport on wind-driven dust. In addition, soil erosion, riverine transport, and volatilization from water represent possible release processes of OCPs in soils. In contrast to primary emissions, the atmospheric OCPs released from secondary sources are especially influenced by complex environmental conditions (Hansen et al., 2004; Ma et al., 2005; Tian et al., 2011). There have been several studies regarding the fates of atmospheric OCPs in agricultural soil (Tao et al., 2008; Xu et al., 2012) or the remote open ocean (Wurl et al., 2006; Ding et al., 2007, 2009; Galbán-Malagón et al., 2013a). However, there have been few studies focusing on their fates over large areas of the estuarine/coastal environment.

From the 1950s–1980s, China was one of the largest global producers and consumers of OCPs (Wei et al., 2007). Dichlorodiphenyltrichloroethanes (DDTs) and hexachlorocyclohexanes (HCHs) were widely used, mainly as insecticides, due to their high efficacy, low cost, and perhaps ignorance of their environmental impact (Wei et al., 2007). China banned the use of these harmful substances in agriculture in 1983. Following this nationwide ban or restriction of related pesticides for agricultural purposes, studies in China have revealed a decreasing trend of OCPs in the atmosphere (Iwata et al., 1993; Zhang et al., 2002; Lin et al., 2012b).

The Yangtze River is one of the world's largest rivers by water discharge, which delivers 900 billion cubic meters of water and 250 million tons of sediment annually into the East China Sea (ECS), a marginal sea between the Asian mainland and the Western Pacific. Located downwind of mainland China and in an important pathway of the East Asian monsoon to the Pacific Ocean, the ECS is strongly influenced by seasonal prevailing winds, and in winter and spring in particular, the prevailing northwest wind from East Asia can bring high loadings of dust (Gao et al., 1997; Hsu et al., 2009). Previous reports from Huaniao Island (HNI) (N30.86°, E122.67°) ~100 km off the Yangtze River mouth in the ECS revealed patterns of seasonal variation in polycyclic aromatic hydrocarbons (PAHs) (Wang et al., 2014) and polybrominated diphenyl ethers (PBDEs) (Li et al., 2015) in PM2.5 (particulate matter < 2.5 μm in diameter), and confirmed a strong influence of continental outflow in cold seasons. In the present study, atmospheric OCPs were examined over HNI (Fig. 1). A total of 160 (80 paired) PM2.5 and polyurethane foam (PUF) samples were collected at HNI for four seasons to determine the seasonal variations in both PM2.5-bound and gaseous OCPs at this receptor site, emphasizing 1) the possible sources of these chemicals under a regime of declining primary and increasing secondary sources, and 2) the characteristics of the seasonal variation and the main influencing factors on particulate and gaseous OCPs over estuarine/coastal areas in the ECS.

2. Materials and methods

2.1. Sampling

PM2.5 and gaseous samples were collected simultaneously using a sampler calibrated at 300 L/min (Guangzhou Mingye Environmental Technology Company, Guangzhou, China). This sampler was designed with a specific inlet to ensure that the collected particles had a diameter of less than 2.5 μm. A pre-combusted quartz filter (20 × 25 cm^2, 0.7 μm, 2600QAT; Pall, Port Washington, NY) was used to capture PM2.5. A solvent-cleaned PUF plug (length 8.0 cm, diameter 6.25 cm, density 0.035 g/cm^3) was used to capture the compounds in the gaseous phase. The air flow was passed through the quartz filters first to collect PM2.5 and then through the PUF to collect gaseous organic contaminants. The time to collect a paired sample (PM2.5 + PUF) was ~23.5 h. Two parallel operational sample blanks were run for each season. A total of 80 paired PM2.5 and PUF samples were taken at HNI during the periods 23 Oct – 8 Nov 2011 (autumn, $n = 16$), 24 Dec 2011–14 Jan 2012 (winter, $n = 20$), 29 Mar – 22 Apr 2012 (spring, $n = 24$), and 24 Jul – 16 Aug 2012 (summer, $n = 20$) (Fig. 1). The island has an area of 3.28 km^2, and is ~66 km from the mainland coastline. Residents on the island (<1000) live mainly from fishing, and therefore local pesticide emissions are almost zero. The sampler was placed on the roof of a three-story building located on the northeast corner of the island at an elevation of ~50 m above sea level.

Before collecting samples, the quartz filters were wrapped in aluminum foil and combusted at 450 °C for 12 h in a muffle furnace. The PUFs were Soxhlet extracted for 48 h with acetone and dichloromethane (DCM), respectively. After removal from the extraction facilities, the PUFs were dried in vacuum desiccators, wrapped in aluminum foil, and stored in an aluminum box. After sampling, the quartz filters were wrapped in baked aluminum foil, and packaged in polyethylene bags, and the PUFs were packed with baked aluminum foil, covered with polyethylene bags, and sealed in an aluminum box. Meteorological data were also recorded simultaneously. Samples were taken to the laboratory and stored at −20 °C until analysis.

2.2. Sample analysis

The samples were Soxhlet extracted for 48 h using DCM. 2,4,5,6-Tetrachloro-*m*-xylene (TCmX) and decachlorobiphenyl (PCB209) were spiked into the extracts as surrogate recovery. After extraction, the reagent was concentrated by rotary evaporation to 5 mL. Hexane was added to the extracts and they were further concentrated to 2 mL using a vacuum rotary evaporator to change the solvent into hexane. The concentrated extracts were purified in an alumina/silica column (8 mm in diameter). The column was packed with 3 cm of deactivated neutral alumina, 3 cm of deactivated neutral silica gel, and 1 cm of anhydrous sodium sulfate from the bottom to the top. The deactivated neutral alumina, deactivated neutral silica gel, and anhydrous sodium sulfate were Soxhlet extracted with DCM for 48 h, and baked in a muffle furnace at increasing temperatures of 250 °C, 180 °C, and 450 °C before use. The column was subsequently eluted with 20 mL of 1:1 DCM and hexane by volume. The effluent was concentrated to 0.5 mL under a gentle steam of nitrogen gas, and spiked with 1 ng of pentachloronitrobenzene as an internal standard.

The OCPs were analyzed using a gas chromatography/mass selective detector (GC-MSD) (Agilent 5975; Agilent Technologies, Santa Clara, CA) The parameters of the capillary column were as follows: CP-Sil 8 CB model; length, 50 m; diameter, 0.25 mm; and film thickness, 0.25 μm. The oven operating conditions were: initial temperature, 60 °C; final temperature, 290 °C; hold time, 10 min; and heating rate, 4 °C/min. Samples (1 μL) were injected into the device at an injector temperature of 250 °C. A standard solution of OCPs, including α-HCH, β-HCH, γ-HCH, *p,p′*-dichlorodiphenyldichloroethane (*p,p′*-DDD), *p,p′*-dichlorodiphenyldichloroethylene (*p,p′*-DDE), *o,p′*-dichlorodiphenyltrichloroethane (*o,p′*-DDT), *p,p′*-DDT, *trans*-chlordane (TC), *cis*-chlordane (CC), α-endosulfan, β-endosulfan, heptachlor, aldrin, dieldrin, and endrin was purchased from AccuStandard, Inc. (New Haven, CT).

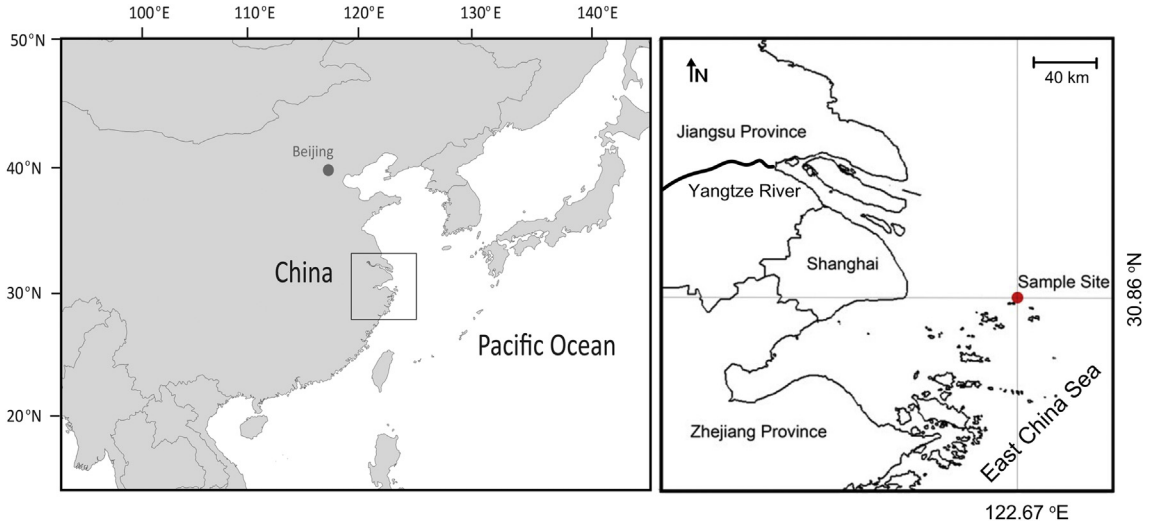

Fig. 1. Map of sampling site at HNI in the ECS.

2.3. Quality assurance and quality control (QA/QC)

Strict regulations were implemented during the experiment to reduce the operating errors. Three laboratory blanks and parallel operational sample blanks were analyzed in the same manner as the samples prior to sample analysis. The compounds that were below the method detection limit (MDL, 0.15–0.24 pg/m^3) were considered as not detected (ND). The target compounds were under the MDL in the blanks. The breakthrough of PUF sample was tested by two consecutive PUF plugs. The results indicated that the target compounds were under the MDL from the subjacent PUF plug. The recoveries of TCmX and PCB209 were 61% ± 23% and 75% ± 22% in the PUF samples and 57% ± 15% and 84% ± 10% in the PM2.5 samples, respectively. The data were corrected according to the mean surrogate recoveries of TCmX and PCB209.

2.4. Principal component analysis – multiple linear regression (PCA-MLR)

Principal component analysis (PCA) is a multivariate analysis method that can extrapolate the relationships between different variants by dimension reduction. Several factors can subsequently be divided by a certain factor interrelation. Multiple linear regression (MLR) can be used to determine the mass apportionment of each designated nonlinear related source factor. To ensure nonlinearity, standardized PCA factor scores are selected as independent variables and standardized concentrations are defined as dependent variables in the calculation. PCA-MLR was performed on the OCPs using IBM SPSS Statistics 19 (SPSS, Chicago, IL).

2.5. Clausius–Clapeyron plot

A Clausius–Clapeyron plot was applied to test the correlation between temperature and gaseous OCPs. The Clausius–Clapeyron equation is:

$$\ln P = (-\Delta H/R)(1/T) + \text{constant} = m\,(1/T) + b,$$

where P is the partial pressure of a specific OCP (Pa), ΔH is the environmental phase transition enthalpy of the OCP (kJ/mol), R is the gas constant (8.314 J/mol), and T is the atmospheric temperature (K). The gaseous phase concentrations of specific OCPs were calculated as partial pressures, and temperature was recorded by in situ measurement. Generally, the slope m was negative, suggesting that the concentration will increase with increasing temperature.

2.6. Logarithmic particle–gas partition coefficient (log K_p) versus logarithmic sub-cooled liquid vapor pressure (log P_L^0)

The $\log K_p - \log P_L^0$ model is able to define the gas-particle partition of POPs. This model uses the following equation (Ma et al., 2011):

$$\log K_p = m_r \log P_L^0 + b_r$$

where m_r and b_r are constants, P_L^0 (Pa) is the sub-cooled liquid vapor pressure and is adjusted by temperature dependency from the model of Paasivirta et al. (1999), and K_p (m^3/μg) is the gas–particle partition coefficient, given by:

$$K_p = (F/P)/A$$

where F (pg/m^3) is the particle concentration of OCPs, A (pg/m^3) is the gas concentration of OCPs, and P (μg/m^3) is the mass concentrations of particles. Theoretically, m_r close to −1 reflects equilibrium conditions; however, a deviation of m_r from −1 can also reflect a true equilibrium state, and m_r is a characteristic parameter only for the specific sorption process (Goss and Schwarzenbach, 1998).

3. Results and discussion

3.1. Concentration levels

Eleven OCPs (α-HCH, β-HCH, γ-HCH, *p,p′*-DDD, *p,p′*-DDE, *o,p′*-DDT, *p,p′*-DDT, TC, CC, α-endosulfan, and β-endosulfan) were detected. The individual OCP concentrations and the PM2.5/(PM2.5 + gaseous phase) ratios for the four seasons are listed in Table 1.

In PM2.5, HCHs exhibited the second highest concentration (4.12 ± 4.76 pg/m^3, ND – 22.56), with an annual mean of 0.16 ± 0.17 (ND – 1.61) pg/m^3 for α-HCH, and 3.36 ± 4.23 (ND – 20.70) pg/m^3 for γ-HCH; while the gaseous HCH concentrations (45.48 ± 19.67 pg/m^3, ND – 97.26) were the highest in all gaseous OCPs, with averages of 4.34 ± 2.63 (0.67–10.34) pg/m^3 for α-HCH,

Table 1
PM2.5 and gas concentrations and their ratios of PM2.5/(PM2.5 + Gas) in HNI.

	Autumn			Winter			Spring			Summer		
	PM2.5	Gas	PM2.5/Total	PM2.5	Gas	PM2.5/Total	PM2.5	Gas	PM2.5/Total	PM2.5	Gas	PM2.5/Total
	(pg/m^3)	(pg/m^3)	(%)	(pg/m^3)	(pg/m^3)	(%)	(pg/m^3)	(pg/m^3)	(%)	(pg/m^3)	(pg/m^3)	(%)
α-HCH	ND–0.37	6.44–9.72	ND – 4.5	ND – 1.61	1.32–2.78	ND – 24.6	ND – 0.40	1.33–10.35	ND – 10.1	ND – 0.09	0.67–5.66	ND – 0.6
	(0.22 ± 0.12)	(8.43 ± 1.20)	(2.6 ± 1.5)	(0.28 ± 0.48)	(1.83 ± 0.42)	(7.1 ± 9.9)	(0.14 ± 0.14)	(5.23 ± 2.64)	(3.0 ± 3.5)	(0.01 ± 0.03)	(2.49 ± 1.59)	(0.1 ± 2.6)
γ-HCH	ND – 3.16	5.14–58.53	0–22.2	3.85–20.70	10.96–24.33	16.6–65.4	ND	1.32–37.98	–	ND	0.70–8.07	–
	(1.27 ± 0.99)	(29.67 ± 16.31)	(5.9 ± 7.0)	(11.61 ± 5.38)	(17.79 ± 4.33)	(37.5 ± 16.1)	ND	(9.49 ± 11.42)	–	ND	(4.12 ± 2.53)	–
op′-DDT	ND – 0.46	ND – 1.84	ND – 20.0	ND – 6.23	ND – 1.18	36.1–100	ND – 0.90	ND – 8.60	ND – 100	ND	0.46–13.41	–
	(0.06 ± 0.16)	(0.35 ± 0.69)	(10.0 ± 14.2)	(2.47 ± 2.04)	(0.25 ± 0.43)	(86.6 ± 24.6)	(0.16 ± 0.32)	(2.91 ± 3.33)	(30.0 ± 48.3)	ND	(5.16 ± 4.18)	–
pp′-DDT	ND – 3.15	ND – 2.32	ND – 100	1.25–6.72	1.63–3.30	32.1–79.2	ND – 1.50	ND – 5.74	ND – 44.5	ND – 1.42	0.92–18.03	ND – 47.0
	(1.90 ± 1.03)	(1.10 ± 0.99)	(63.5 ± 35.2)	(3.10 ± 1.91)	(2.27 ± 0.52)	(52.3 ± 14.8)	(0.43 ± 0.65)	(2.17 ± 1.47)	(11.5 ± 17.1)	(0.60 ± 0.57)	(5.81 ± 4.96)	(16.4 ± 18.3)
pp′-DDE	0.19–0.60	6.21–11.34	2.8–8.8	0.15–1.18	0.71–2.19	11.2–43.1	0.43–1.30	2.97–15.04	4.6–20.3	0.23–0.77	3.03–26.50	1.8–18.9
	(0.45 ± 0.13)	(8.25 ± 2.12)	(5.3 ± 2.1)	(0.57 ± 0.33)	(1.60 ± 0.49)	(23.5 ± 9.4)	(0.80 ± 0.24)	(7.04 ± 3.13)	(11.5 ± 4.8)	(0.58 ± 0.19)	(9.86 ± 6.88)	(8.2 ± 6.2)
pp′-DDD	0.86–2.24	1.17–5.42	18.1–57.3	2.49–6.96	ND – 2.49	65.1–100	0.73–3.74	3.22–8.16	11.8–44.1	1.68–3.87	0.91–15.83	9.6–71.9
	(1.49 ± 0.47)	(2.44 ± 1.46)	(40.8 ± 13.8)	(4.95 ± 1.37)	(0.99 ± 0.81)	(83.2 ± 13.3)	(2.06 ± 0.93)	(5.18 ± 1.47)	(28.5 ± 10.7)	(2.48 ± 0.63)	(8.07 ± 4.27)	(28.7 ± 17.7)
TC	ND – 1.74	ND – 5.18	ND – 100	1.69–7.69	ND – 4.55	48.1–100	ND – 2.26	0.69–3.64	ND – 76.1	ND – 0.87	0.23–10.64	ND – 26.6
	(0.82 ± 0.51)	(2.86 ± 1.65)	(30.7 ± 30.3)	(3.35 ± 1.71)	(1.34 ± 1.23)	(71.6 ± 16.2)	(1.07 ± 0.79)	(1.93 ± 1.01)	(35.7 ± 25.7)	(0.10 ± 0.27)	(5.97 ± 3.48)	(3.3 ± 8.5)
CC	0.24–0.66	5.07–11.71	2.1–5.8	0.83–2.51	0.35–1.16	46.7–100	0.37–2.07	0.36–8.98	6.0–78.3	ND – 0.53	1.14–15.19	0–21.3
	(0.44 ± 0.15)	(9.78 ± 2.29)	(4.3 ± 1.1)	(1.30 ± 0.46)	(0.77 ± 0.31)	(64.0 ± 12.1)	(1.04 ± 0.53)	(4.34 ± 3.07)	(29.4 ± 28.0)	(0.25 ± 0.17)	(6.08 ± 4.48)	(6.5 ± 7.9)
α- endosulfan	ND	ND – 2.29	–	ND – 2.70	ND – 0.69	ND – 100	ND – 1.08	0.68–3.27	ND – 41.6	ND – 0.33	0.83–13.30	ND – 2.6
	ND	(1.28 ± 0.90)	–	(0.33 ± 0.80)	(0.13 ± 0.24)	(48.3 ± 50.1)	(0.17 ± 0.30)	(1.68 ± 0.70)	(9.9 ± 13.3)	(0.05 ± 0.11)	(6.65 ± 4.45)	(0.5 ± 1.1)
β- endosulfan	0.24–0.90	0.67–5.00	13.7–40.7	ND – 2.18	ND – 5.37	ND – 100	ND – 1.36	ND – 14.31	ND – 100	ND – 0.51	1.37–7.01	ND – 16.8
	(0.61 ± 0.24)	(2.16 ± 1.44)	(24.6 ± 9.3)	(0.91 ± 0.70)	(1.03 ± 1.62)	(58.6 ± 39.3)	(0.60 ± 0.39)	(3.79 ± 4.13)	(25.8 ± 29.1)	(0.12 ± 0.20)	(4.10 ± 1.71)	(3.9 ± 6.4)

nd = no detected.

and 14.26 ± 10.44 (0.70–58.53) pg/m^3 for γ-HCH. The concentrations were significantly lower than those in adjacent regions, such as the South China Sea (67 ± 33 pg/m^3 for α-HCH, and 771 ± 310 pg/m^3 for γ-HCH (Zhang et al., 2007)), Singapore (104.17 ± 17.50 pg/m^3 for α-HCH, and 88.66 ± 34.87 pg/m^3 for γ-HCH (He et al., 2009)), the China marginal seas (13 ± 8.1 pg/m^3 for α-HCH, and 110 ± 76 pg/m^3 for γ-HCH (Lin et al., 2012b)), Taihu Lake (74 ± 45 pg/m^3 for α-HCH, and 46 ± 24 pg/m^3 for γ-HCH (Qiu et al., 2004)), and Korea background sites (11–542 pg/m^3 for HCHs (Jin et al., 2013)). They were comparable to those observed in the Indian Ocean (3.2 pg/m^3 for α-HCH, and 13.8 pg/m^3 for γ-HCH (Wurl et al., 2006)) and the Atlantic Ocean (3 pg/m^3 for α-HCH and 22 pg/m^3 for γ-HCH (Jaward et al., 2004)).

DDTs were the most abundant species in PM2.5 (5.71 ± 3.91 pg/m^3) and the second most abundant species in the gaseous phase (15.73 ± 12.10 pg/m^3). The annual mean concentration of *o,p′*-DDT was 0.72 ± 0.99 pg/m^3 in PM2.5, and 2.30 ± 2.54 pg/m^3 in the gaseous phase, and it was 1.48 ± 1.15 pg/m^3 for *p,p′*-DDT in PM2.5, and 2.89 ± 1.83 pg/m^3 in the gaseous phase. These concentrations were comparable to those in the China marginal seas (19 ± 15 pg/m^3 for *o,p′*-DDT, and 5.1 ± 5.1 pg/m^3 for *p,p′*-DDT (Lin et al., 2012b)), Korea background sites (ND of 56.5 pg/m^3 for DDTs (Jin et al., 2013)), and the Indian Ocean (5.9 pg/m^3 for *p,p′*-DDT (Wurl et al., 2006)); but significantly lower than those in the South China Sea (196 ± 141 pg/m^3 for *o,p′*-DDT, and 58 ± 65 pg/m^3 for *p,p′*-DDT (Zhang et al., 2007)) and Tai Lake (767 ± 712 pg/m^3 for *o,p′*-DDT, and 124 ± 91 pg/m^3 for *p,p′*-DDT (Qiu et al., 2004)) measured 10 years ago. The annual mean concentrations of *p,p′*-DDE were 0.62 ± 0.21 pg/m^3 in PM2.5 and 6.63 ± 3.50 pg/m^3 in the gas phase; while those of *p,p′*-DDD were 2.83 ± 1.30 pg/m^3 in PM2.5 and 4.30 ± 2.74 pg/m^3 in the gaseous phase. These levels were considerably lower compared with other regions in China, such as 212 ± 134 pg/m^3 for *p,p′*-DDE in Taihu Lake (Qiu et al., 2004) and 51 ± 50 pg/m^3 for *p,p′*-DDE in the South China Sea (Zhang et al., 2007), but were slightly higher than those in Singapore (1.94 ± 1.83 pg/m^3 for *p,p′*-DDD (He et al., 2009)) and the Indian Ocean (1.3 pg/m^3 for *p,p′*-DDD (Wurl et al., 2006)).

Chlordanes were the third most abundant species in OCPs over the ECS, with a mean concentration of 9.95 ± 5.00 pg/m^3. The annual mean concentrations were 1.39 ± 1.18 pg/m^3 for TC and 0.80 ± 0.46 pg/m^3 for CC in PM2.5, and 2.98 ± 2.04 pg/m^3 for TC and 4.97 ± 3.68 pg/m^3 for CC in the gaseous phase. These concentrations were comparable to those observed in Korea background sites (ND – 11 pg/m^3 for total chlordanes (Jin et al., 2013)). However, they were higher than those over the Indian Ocean (1.2 pg/m^3 for TC and 0.5 pg/m^3 for CC (Wurl et al., 2006)) and the Atlantic Ocean (0.14 pg/m^3 for TC and 0.4 pg/m^3 for CC (Lohmann et al., 2009)). These observations suggest the possible continued usage of chlordanes in China.

Endosulfans had the lowest concentrations (5.90 ± 5.02 pg/m^3) among all OCPs detected in both the gaseous and particulate phases. The mean concentrations of α-endosulfan were 0.57 ± 0.41 pg/m^3 in PM2.5 and 2.85 ± 2.13 pg/m^3 in the gaseous phase. The annual use of technical endosulfan in China increased to 2800 t/y from 1998 to 2004, and technical endosulfan was prohibited in July 2011 (Jia et al., 2009; Weber et al., 2010). Technical endosulfan was most frequently applied to cotton in North China, and the usage for cotton reached ~56% of the total consumption (Jia et al., 2009). The half-life of endosulfan in the environment is relatively short compared with other OCPs, such as DDT and chlordanes (Weber et al., 2010). The low endosulfan concentration with poorly defined seasonal variation observed in our study was consistent with relatively low endosulfan usage in the regions adjacent to the ECS and its rapid degradation.

3.2. Sources identified using isomer ratios

The main sources of HCHs include the historical usage of technical HCH and lindane. The consumption of technical HCH in China was estimated at approximately 4–4.46 million tons before 1983 and that of lindane at approximately 3200 tons between 1991 and 2000 (Li et al., 1998; Li, 1999; Qiu et al., 2004). Technical HCH is a mixture of several HCH isomers, consisting of 55%–80% α-HCH, 5%–14% β-HCH, 8%–15% γ-HCH, and 2%–16% δ-HCH, while lindane consists of >95% γ-HCH by mass (Rodriguez-Garrido et al., 2010). Generally, the α-/γ-HCH ratio is applicable for identifying the sources and residual times (Li and Bidleman, 2003; Qiu et al., 2004; Lin et al., 2012a). The ratios of α-/γ-HCH were 0.12 ± 0.26 in PM2.5 and 0.69 ± 0.91 in the gaseous phase (Fig. 2). The lower α-/γ-HCH ratios found in our study indicate the influence of lindane usage in adjacent terrestrial regions. This is consistent with the continued use of lindane after the phase-out of technical HCH in China. The α-/γ-HCH ratios in the gaseous phase showed well-defined seasonal variation, with considerably lower ratios in winter and autumn compared to spring and summer (0.25 ± 0.31 versus 1.06 ± 1.07, respectively), which coincided with higher concentrations of γ-HCH in winter and autumn. The high input of γ-HCH was probably derived from the residual lindane brought in via upwind agriculture soils when air masses from the China mainland reached the area. As γ-HCH has a lower Henry's Law Constant than α-HCH and γ-HCH can undergo phototransformation into α-HCH (Oehme, 1991), γ-HCH has a shorter atmospheric lifetime than α-HCH. All of these properties lead to a lower residence time for γ-HCH in the atmosphere compared to that of α-HCH. As a result, the higher α-/γ-HCH ratios could indicate that the HCHs had undergone longer exposure to the environment due to long-range transport from the remote open ocean area. This is also consistent with the lower levels of both α-HCH and γ-HCH in the gaseous phase, especially in summer.

The ratio of (*p*,*p*′-DDE + *p*,*p*′-DDD)/*p*,*p*′-DDT is an indicator of the residence time of DDTs in the environment because *p*,*p*′-DDT can degrade slowly into *p*,*p*′-DDE and *p*,*p*′-DDD. A ratio >1 indicates the occurrence of significant degradation in the DDT residues; while a ratio <1 is considered to reflect fresh DDT input (Hitch and Day, 1992; Li et al., 2006). The difference between the ratios of the particulate and gaseous phases was significant (4.44 in the gaseous phase versus 1.35 in PM2.5) (Fig. 3). The higher ratio of (*p*,*p*′-DDE + *p*,*p*′-DDD)/*p*,*p*′-DDT in the gaseous phase indicates that they were mainly composed of degradation products. This is consistent with the ban of DDTs in agriculture in 1983 (Liu et al., 2009), and present-day DDTs over the ECS mostly originating from volatilization. However, the ratios of (*p*,*p*′-DDE + *p*,*p*′-DDD)/*p*,*p*′-DDT in several PM2.5 or gaseous samples from summer and autumn were <1, suggesting fresh input of DDTs.

The ratio of *o*,*p*′-DDT/*p*,*p*′-DDT can be applied to identify the origin of the fresh DDT. Technical DDT and dicofol-type DDT have historically been the major contributors to DDT consumption in China. It was estimated that approximately 460000 tons of technical DDT were produced in China before 1983 (Wei et al., 2007; Liu et al., 2009). After the prohibition of technical DDT, it continued to be used under certain circumstances, including malaria control, mosquito repellency, and in antifouling paints (Wei et al., 2007; Lin et al., 2009). Dicofol products, possessing 3%–7% DDTs as impurities, came into use after the prohibition of technical DDT. The total dicofol-type DDT output in China was estimated to be 8770 tons between 1988 and 2002 (Qiu et al., 2005). The ratio of *o*,*p*′-DDT/*p*,*p*′-DDT can be used as an indicator to distinguish between technical DDT and dicofol products (Qiu et al., 2005; Liu et al., 2009). The ratio of *o*,*p*′-DDT/*p*,*p*′-DDT in PM2.5 over the ECS was very low (0.06 ± 0.19) (Fig. 3), suggesting that the fresh DDT was mainly derived from the usage of technical DDT. For the gaseous phase, the ratio of *o*,*p*′-DDT/*p*,*p*′-DDT was 0.10 ± 0.18 with relatively high concentrations of *p*,*p*′-DDT in summer and autumn (especially in July), also indicating that the fresh DDT was derived from technical DDT. However, in winter and spring, the ratio increased (1.57 ± 1.93), mainly due to the declining concentration of *p*,*p*′-DDT, indicating that there was no new application of technical DDT. It is worth noting that there was new input of technical DDT in summer and autumn during the sampling period. To promote sustainability

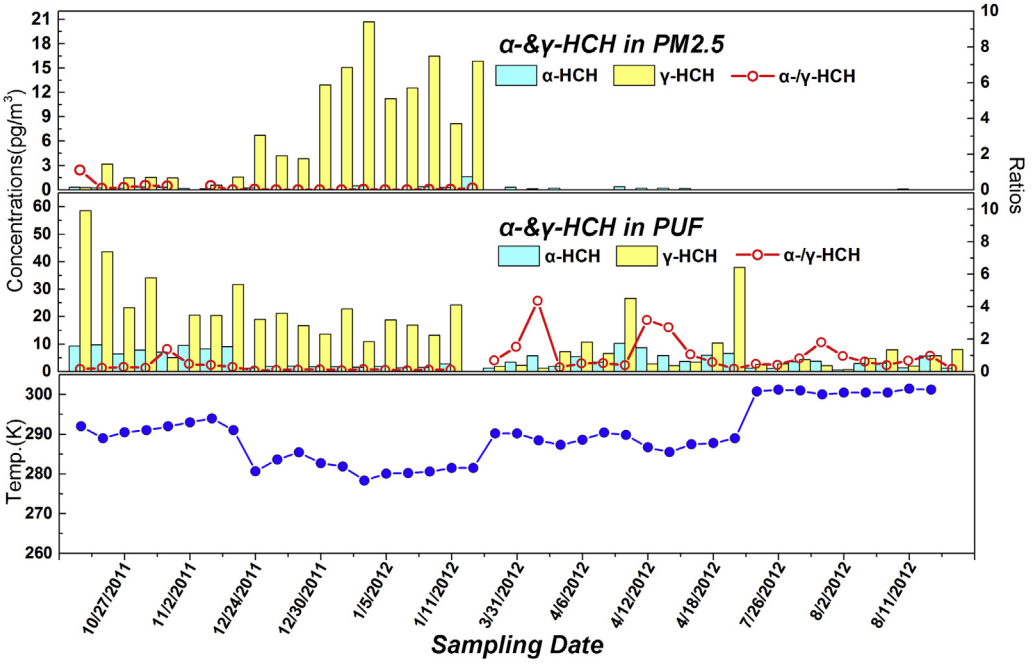

Fig. 2. Temporal variation of isomer concentrations of HCHs and ratio of α-/γ-HCH in PM2.5 and gaseous phase samples at HNI in the ECS.

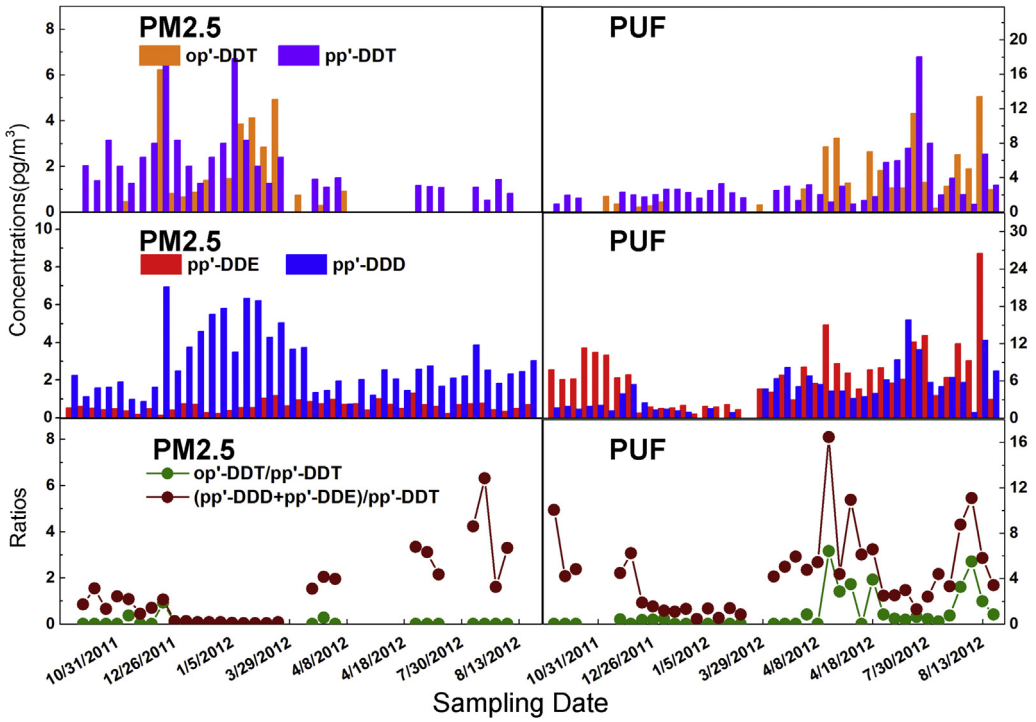

Fig. 3. Temporal variation of isomer concentrations of DDTs and ratios of o,p′-DDT/p,p′-DDT and (p,p′-DDE + p,p′-DDD)/p,p′-DDT in PM2.5 and gaseous phase samples at HNI in the ECS.

in the fishery industry, the Chinese government implements a strict "no fishing policy" from June 1st to September 1st each year. During the fishing ban season, all fishing activities are forbidden and fishing boats are harbored at port where many of them undergo maintenance, including repainting with antifouling paints (Lin et al., 2009). These paints contain small amounts of technical DDT to prevent biofouling. Thus, stripping and repainting of the antifouling paints during the frequent boat maintenance activities may explain the existence of a new source of *p,p′*-DDT, especially in summer and autumn, associated with technical DDT (Lin et al., 2009).

Chlordane was widely used as a termiticide against ants in tropical and subtropical timber. The total estimated production of technical chlordane in China was approximately 3431 tons from 1988 to 2008 (Wang et al., 2012). Technical chlordane was banned for all purposes in 2009 (Wang et al., 2012). The TC/CC ratio is commonly used to elucidate the sources of chlordanes in the environment. In general, the ratios of TC/CC range between 1.2 and 1.5 in the technical chlordane products (Li et al., 2007), while this ratio would gradually decrease in the environment because the degradation rate of TC is faster than that of CC (Bidleman et al., 2002; Cheng et al., 2007). The ratios of TC/CC showed a slight difference between the gaseous and particulate samples (1.01 ± 1.02 versus 1.44 ± 1.17, respectively), and both ratios were close to the original ratios in the products (Fig. 4). This suggests that the new application of technical chlordanes was primarily responsible for the current levels of chlordanes in the atmosphere over the ECS. In PM2.5, the ratios of TC/CC in winter (1.62 ± 1.05) were much higher than those in other seasons (0.66 ± 0.63), and the concentrations were also significantly higher in winter. Residual chlordane in upwind agricultural soil was still fresh, suggesting recent new application. Similarly, in the gaseous phase, both higher concentrations and higher TC/CC ratios (1.50 ± 1.44) were observed in summer. Although the air mass over HNI was mainly derived from Southeast Asia or the remote open ocean, there appeared to have been new application of chlordanes in nearby coastal areas in summer. Between 1988 and 2008, the total chlordane usage in China was 2745 tons, accounting for approximately 80% of total national production in this period, and Zhejiang Province on the East China coast (directly facing the sampling region) was the largest consumer in the country. As China prohibited the technical usage of chlordanes in 2009, it is reasonable to suppose that there may still be some illegal usage of these substances in the surrounding areas of the ECS.

As the widespread use of DDTs and HCHs was prohibited in China in the early 1980s, the current presence of DDTs and HCHs in the atmosphere is considered to be predominantly derived from the residual chemicals from historical usage. One possibility is that weathered agricultural soils may serve as continuing sources after the ban on the use of these substances in agricultural production. Moreover, the higher ratios of α-/γ-HCH, (*p,p′*-DDE + *p,p′*-DDD)/*p,p′*-DDT and CC/TC in the gaseous compared to the particulate phase also confirmed that gaseous OCPs were preferentially degraded compared to particulate phase OCPs when exposed to the atmosphere.

3.3. Seasonal variation and dominant factors identified by PCA

PCA combined with $\log K_p - \log P_L^0$ and Clausius–Clapeyron plots was performed to reveal the seasonal variation, and to investigate the factors influencing OCPs over the ECS. First, the covariance method was performed for PCA, which was used to divide the samples into groups that had similar sample scores. After performing PCA on the datasets containing these OCP compounds in PM2.5, the score plot of eigenvalues >1 indicated that 69% of the variance in the data could be explained by the first two components (Fig. 5A). The first principal component (PC1), primarily composed of samples from spring, summer, and autumn, accounted for 42% of

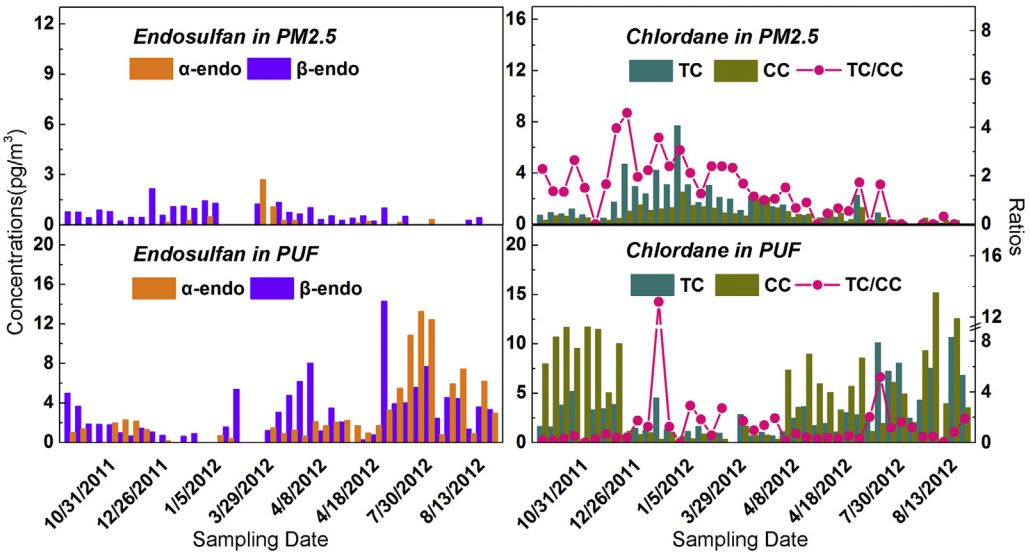

Fig. 4. Temporal variation of isomer concentrations of chlordanes and endosulfans and ratio of TC/CC in PM2.5 and gaseous phase samples at HNI in the ECS.

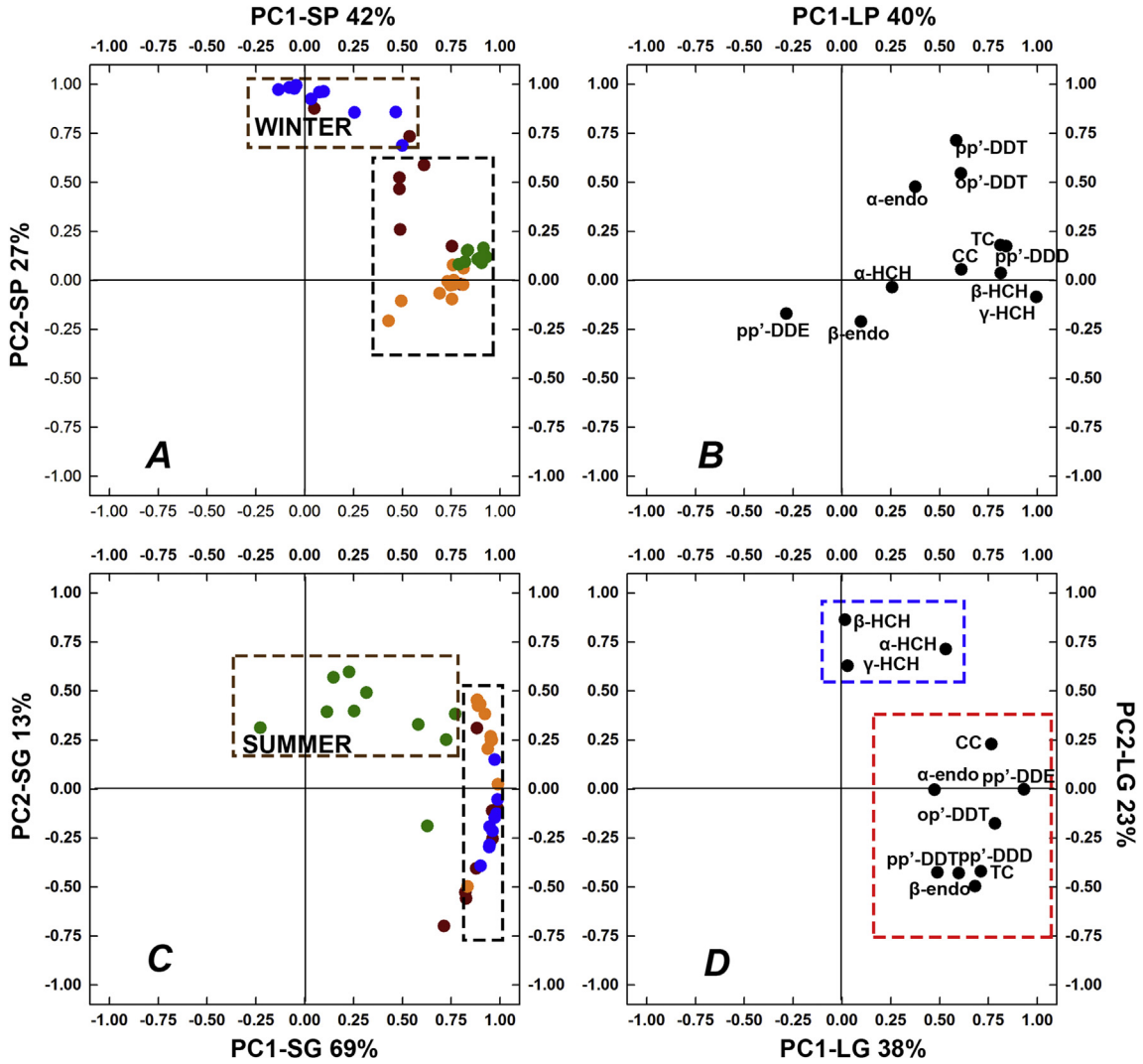

Fig. 5. Factor scores (A) and factor loadings (B) of the particulate OCPs, and factor scores (C) and factor loadings (D) of the gaseous OCPs using the PCA of eleven OCPs from PM2.5 and gaseous phase samples at HNI in the ECS.

the total variance. The second principal component (PC2, 27%) was highly weighted on the winter samples. The inconsistency between winter and other seasons was seen not only in the sample score results by PCA, but was also indicated by the seasonal differences in PM2.5-bound concentrations and ratios of PM2.5/(PM2.5 + gaseous phase). The seasonal variations in PM2.5-bound concentrations of individual OCPs are shown in Figs. 2–4. For HCHs, DDTs, and chlordanes, the PM2.5-bound concentrations were highest in winter. The mean PM2.5 concentration for the measured OCPs in winter was 31.89 ± 8.78 pg/m^3, which was approximately 3-fold higher than those for the other three seasons (9.16 ± 3.63 pg/m^3). The ratios of PM2.5/(PM2.5 + gaseous phase) are listed in Table 1. HCHs, DDTs, chlordanes, and endosulfans were mostly concentrated in the gaseous phase, except in winter, and the average ratio of PM2.5/(PM2.5 + gaseous phase) in winter (64% ± 14%) was significantly higher than those in other seasons (8% ± 2% in autumn, 10% ± 6% in spring, and 8% ± 4% in summer). In winter, the highest PM2.5-bound concentration corresponded with PM2.5/(PM2.5 + gaseous phase), indicating significant input of particulate-phase OCPs. In previous studies using back-traced air mass trajectories, continental outflow was shown to be a key factor influencing the concentrations of PBDEs, PAHs, organic carbon, and elemental carbon in PM2.5 and total suspended particles detected in the pathway of the East Asian monsoon (Guo et al., 2004; Wang et al., 2014; Li et al., 2015). The East Asian monsoon can bring large quantities of particulate OCPs to the ECS adsorbed on dust particles. However, the relatively low concentrations of gaseous OCPs observed during the prevailing northwest monsoon in winter were likely due to low volatilization from soils associated with low temperatures and low residual levels in the agricultural soils more than two decades after their prohibition. In addition, soils with high total organic carbon content also have a large retention capacity for OCPs, which reduces their volatilization from the soil (Tian et al., 2011, 2012; Xu et al., 2012).

PCA was also performed in terms of compound loadings, and only one PC (eigenvalue > 1) was extracted (Fig. 5B). The PC1 of compound loading for the PM2.5 samples, accounting for 40% of the total variance, was characteristic of the β-HCHs, γ-HCH, and *p*,*p*′-DDD that were widely detected as residual substances in agricultural soils. Although the samples from winter were separated from other seasons by the results from the sample scores, no specific compound was found separating winter and other seasons. It is possible that weathered agricultural soils transported by continental outflow represented the dominant source of PM2.5-bound OCPs over the ECS.

The MLR method was performed using the standardized PM2.5-bound concentrations as the dependent variables and the standardized factor scores as the independent variables. The compound loadings revealed that PC1 contributed up to 83% of the seasonal variation of PM2.5-bound concentrations. This provided further indication that the significantly higher annual contribution of the particulate OCPs over the ECS occurred mainly in winter.

PCA identified two PCs based on the scores of the gaseous samples, which accounted for 82% of the total variance (Fig. 5C). PC1 (69%) was weighted on samples from autumn, winter, and spring. PC2 (13%) was mainly weighted on summer samples, suggesting significant differences between summer and the other seasons. PCA of the compound loadings was performed to investigate the separation of compound groups (Fig. 5D). The results showed that DDTs, chlordanes, and endosulfans were the primary contributors to PC1 (38%), while HCHs mostly contributed to PC2 (23%). As shown in Figs. 2–4, DDTs, chlordanes, and endosulfans in the gaseous phase showed peak concentrations in autumn or summer, whereas the highest concentration of gaseous HCHs occurred in winter. The gas–particle partition model was applied to test the relationship between particulate OCPs and gaseous OCPs. The plot of log K_p versus log P_L^0 is shown in Fig. 6. For each OCP, a slope that deviates from −1 indicates a non-equilibrium state of gas-particle partition. However, numerous field measurements indicated a deviation of m_r from −1, and proposed the existence of equilibrium even when the slope is not −1 (Galbán-Malagón et al., 2013b; Berrojalbiz et al., 2014). Therefore, the correlation between log K_p and log P_L^0 was checked for each OCP in the samples (Fig. 6). Weak linear correlations between log K_p and log P_L^0 were observed for DDTs and chlordane, indicating that they were affected by large-scale unstable seasonal sources. There are multiple possible explanations for the high levels of *p*,*p*′-DDT and chlordane in the gaseous phase in autumn and summer, including volatilization from agricultural soils and/or volatilization from coastal waters. Previous studies, including those performed in the Pearl River Delta, large Indian cites, and background sites in Korea (Li et al., 2007; Chakraborty et al., 2010; Jin et al., 2013), indicated that gaseous OCPs were positively correlated with the temperature in the atmosphere, and were mainly associated with volatilization from agricultural soils. As the sampling area was surrounded by the ocean and there was almost no local historical pesticide use on the island, the OCP volatilization was most likely derived from the ocean rather than the adjacent soils. Lin et al. (2012b) reported that CC and TC showed net volatilization fluxes out of the water in a coastal area. Technical chlordane was mainly used for termite control in residential and commercial buildings, as well as in forests using a surface soil burial method. Thus, it would be more inclined to enter coastal waters via runoff (García-Flor., 2009; Lin et al., 2012b). Furthermore, it has been estimated that the Yangtze River discharges ~87% of its annual sediments and water in the June–October flood season (Xu and Milliman, 2009), and large amounts of OCPs from the Yangtze River discharge are capable of sustaining high water fugacity in the area, resulting in enhanced water fugacity and significant net volatilization during the flood and warm seasons. In addition, the high levels of gaseous-phase *p*,*p*′-DDT and chlordane in autumn and summer may be explained by short-term application of pesticides, especially the technical DDTs and chlordanes, in adjacent terrestrial regions in these seasons. As discussed above, there continues to be a fresh source of *p*,*p*′-DDT from antifouling paints, especially in summer and autumn during the fishing ban season. Higher ratios of TC/CC and higher concentrations in the gaseous phase in summer suggest that there continues to be illegal usage of the banned chlordanes in the surrounding areas of the ECS. In contrast, there was a strong linear correlation between log K_p and log P_L^0 for α-HCH and γ-HCH with $r^2 = 0.74$ and $r^2 = 0.70$, respectively, indicating that they were close to equilibrium. Unlike DDTs and chlordanes, HCHs have been prohibited for more than 30 years globally, and therefore there are almost no primary sources remaining in the environment. HCHs have high volatilities and rates of degradation compared with DDTs and chlordanes. Consequently, HCH residual levels in agricultural soils and water should be low after their long-term prohibition (Iwata et al., 1993; Wang et al., 2005). That is, the levels observed in the present study represent the current background levels in the coastal ECS. Moreover, Clausius–Clapeyron plots (negative slope m) demonstrated that HCH concentrations were not correlated with temperature (Table 2). Thus, the elevated concentrations of gaseous HCHs observed in winter when the East Asian monsoon brings large quantities of particulate HCHs to the ECS indicate that the aerosol concentration is one of the key parameters controlling air–particle partitioning of these semivolatile organic compounds, and that increased levels of HCHs in the particulate phase could cause a partial shift to gaseous HCHs over the ECS in winter.

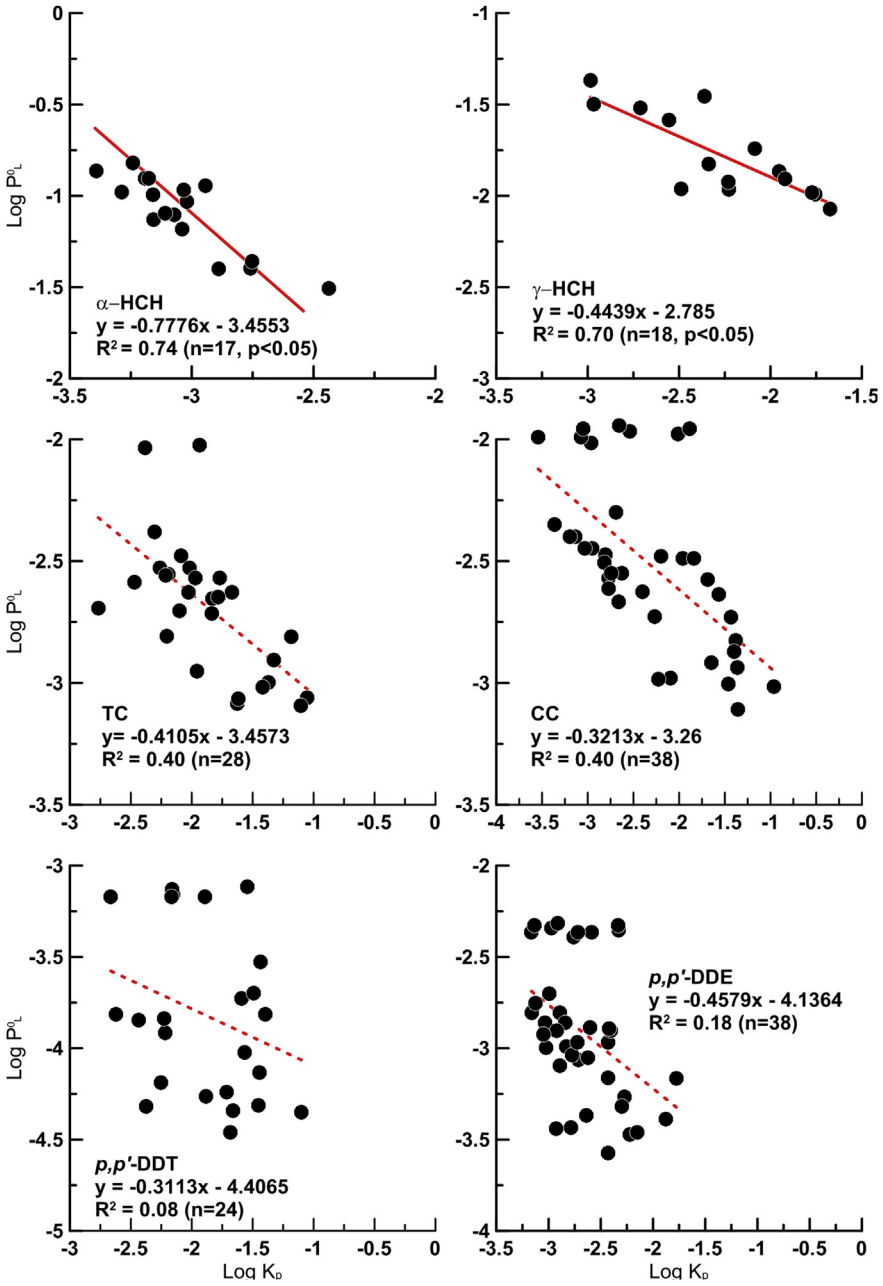

Fig. 6. Log K_p VS log P_L^0 plots of individual OCPs at HNI in the ECS.

Table 2
The result from the Clausius-Clapeyron plots for the OCPs in HNI.

	Clausius-Clapeyron plots				
	Slope	Intercept	r^2	P	△H (kJ/mol)
α-HCH	−1360	−19.66	0.02	>0.05	11.3
γ-HCH	4940	−40.44	0.14	>0.05	−41.1
o,p′-DDT	−18257	35.74	0.28	<0.05	151.8
p,p′-DDT	−3137	−14.57	0.02	>0.05	26.1
p,p′-DDE	−6955	−0.04	0.5	<0.01	57.8
p,p′-DDD	−11904	16.24	0.33	<0.01	99.0
TC	−7665	1.07	0.19	<0.01	63.7
CC	−8344	3.96	0.35	<0.01	69.4
α-endosulfan	−12195	16.35	0.26	<0.05	101.4
β-endosulfan	−18599	37.78	0.47	<0.01	154.6

4. Conclusions

This study presents the first comprehensive data set of atmospheric OCPs over the ECS under a regime of declining primary and increasing secondary sources. The PM2.5-bound OCPs showed strong seasonal variation, with the highest and lowest levels in winter and summer, respectively. It is suggested that the particulate OCPs originated from weathered agricultural soils transported by continental outflow in winter. The gaseous phase exhibited two different patterns of OCPs. The highest levels of DDTs and chlordanes occurred in summer, and the lowest in winter. Currently, illegal usage and net volatilization from the sea surface provide greater contributions to gaseous DDTs and chlordanes in summer. The DDTs and chlordanes in the gaseous phase and aerosols had different sources and input pathways, leading to a non-equilibrium

state in gas–particle partitioning over the ECS. In contrast, the highest levels of HCHs occurred in winter, and the lowest in summer. The lower concentrations of gaseous HCHs observed in summer suggested that net volatilization had a relatively limited impact on gaseous HCHs due to the long-term prohibition of their use and low residual levels in the catchment. The strong linear correlation between log K_p and log P_L^0 for α-HCH and γ-HCH indicated that they were close to equilibrium, suggesting that increased numbers of particulate HCHs could cause a partial shift to gaseous HCHs over the ECS in winter.

Acknowledgments

This work was supported by the Natural Science Foundation of China (NSFC) (No: 41176085), National Basic Research Program of China (No: 2014CB953701) and Shanghai Science and Technology Committee (No: 12DJ1400102). We would like to thank Mr. Fujiang Wang for his help in sample collection. The anonymous reviewers are sincerely appreciated for their critical reviews that greatly improved this paper.

References

Aigner, E.J., Leone, A.D., Falconer, R.L., 1998. Concentrations and enantiomeric ratios of organochlorine pesticides in soils from the US corn belt. Environ. Sci. Technol. 32, 1162–1168.
Becker, S., Halsall, C.J., Tych, W., Kallenborn, R., Schlabach, M., Manø, S., 2012. Changing sources and environmental factors reduce the rates of decline of organochlorine pesticides in the Arctic atmosphere. Atmos. Chem. Phys. 12, 4033–4044.
Berrojalbiz, N., Castro-Jiménez, J., Mariani, G., Wollgast, J., Hanke, G., Dachs, J., 2014. Atmospheric occurrence, transport and deposition of polychlorinated biphenyls and hexachlorobenzene in the Mediterranean and Black seas. Atmos. Chem. Phys. 14, 8947–8959.
Bidleman, T.F., Jantunen, L.M.M., Helm, P.A., Brorstrom-Lunden, E., Juntto, S., 2002. Chlordane enantiomers and temporal trends of chlordane isomers in arctic air. Environ. Sci. Technol. 36, 539–544.
Chakraborty, P., Zhang, G., Li, J., Xu, Y., Liu, X., Tanabe, S., Jones, K.C., 2010. Selected organochlorine pesticides in the atmosphere of major Indian cities: levels, regional versus local variations, and sources. Environ. Sci. Technol. 44, 8038–8043.
Cheng, H., Zhang, G., Jiang, J.X., Li, X., Liu, X., Li, J., Zhao, Y., 2007. Organochlorine pesticides, polybrominated biphenyl ethers and lead isotopes during the spring time at the Waliguan Baseline Observatory, northwest China: Implication for long-range atmospheric transport. Atmos. Environ. 41, 4734–4747.
Dickhut, R.M., Cincinelli, A., Cochran, M., Ducklow, H.W., 2005. Atmospheric concentrations and air-water flux of organochlorine pesticides along the western Antarctic Peninsula. Environ. Sci. Technol. 39, 465–470.
Ding, X., Wang, X.M., Xie, Z.Q., Xiang, C.H., Mai, B.X., Sun, L.G., Zheng, M., Sheng, G.Y., Fu, J.M., 2007. Atmospheric hexachlorocyclohexanes (HCHs) in the North Pacific Ocean and the adjacent Arctic Region: spatial Patterns, chiral signatures and sea-air exchanges. Environ. Sci. Technol. 41, 5204–5209.
Ding, X., Wang, X.M., Wang, Q.Y., Xie, Z.Q., Xiang, C.H., Mai, B.X., Sun, L.G., 2009. Atmospheric DDTs over the North Pacific Ocean and the adjacent Arctic region: spatial distribution, congener patterns and source implication. Atmos. Environ. 43 (28), 4319–4326.
Galbán-Malagón, C.J., Cabrerizo, A., Caballero, G., Dachs, J., 2013a. Atmospheric occurrence and deposition of hexachlorobenzene and hexachlorocyclohexanes in the Southern Ocean and Antarctic Peninsula. Atmos. Environ. 80, 41–49.
Galbán-Malagón, C.J., Del Vento, S., Cabrerizo, A., Dachs, J., 2013b. Factors affecting the atmospheric occurrence and deposition of polychlorinated biphenyls in the Southern Ocean. Atmos. Chem. Phys. 13, 12029–12041.
Gao, Y., Arimoto, R., Duce, R., Zhang, X., Zhang, G., An, Z., Chen, L., Zhou, M., Gu, D., 1997. Temporal and spatial distributions of dust and its deposition to the China Sea. Tellus B 49, 172–189.
García-Flor, N., Dachs, J., Bayona, J.M., Albaigés, J., 2009. Surface waters are a source of polychlorinated biphenyls to the coastal atmosphere of the North-Western Mediterranean Sea. Chemosphere 75, 1144–1152.
Gioia, R., Li, J., Schuster, J., Zhang, Y., Zhang, G., Li, X., Spiro, B., Bhatia, R.S., Dachs, J., Jones, K.C., 2012. Factors affecting the occurrence and transport of atmospheric organochlorines in the China sea and the northern Indian and South east Atlantic Oceans. Environ. Sci. Technol. 46, 10012–10021.
Goss, K., Schwarzenbach, R., 1998. Gas/solid and gas/liquid partitioning of organic compounds: critical evaluation of the interpretation of equilibrium constants. Environ. Sci. Technol. 32, 2025–2032.
Guo, Z.G., Feng, J.L., Fang, M., Chen, H.Y., Lau, K.H., 2004. The elemental and organic characteristics of PM2.5 in Asian dust episodes in Qingdao, China, 2002. Atmos. Environ. 38, 909–919.
Hansen, K.M., Christensen, J.H., Brandt, J., Frohn, L.M., Geels, C., 2004. Modelling atmospheric transport of α-hexachlorocyclohexane in the Northern Hemisphere with a 3-D dynamical model: DEHM-POP. Atmos. Chem. Phys. 4, 1125–1137.
Hitch, R.K., Day, H.R., 1992. Unusual persistence of DDT in some western USA soils. Bull. Environ. Contam. Toxicol. 48, 259–264.
He, J., Balasubramanian, R., Karthikeyan, S., Joshi, U.M., 2009. Determination of semi-volatile organochlorine compounds in the atmosphere of Singapore using accelerated solvent extraction. Chemosphere 75, 640–648.
Hsu, S., Liu, S., Arimoto, R., Liu, T., Huang, Y., Tsai, F., Lin, F., Kao, S., 2009. Dust deposition to the East China Sea and its biogeochemical implications. J. Geophys. Res. 114, D15304.
Iwata, H., Tanabe, S., Sakai, N., Tatsukawa, R., 1993. Distribution of persistent organochlorines in the oceanic air and surface seawater and the role of ocean on their global transport and fate. Environ. Sci. Technol. 27, 1080–1098.
Jaward, F.M., Barber, J.L., Booij, K., Dachs, J., Lohmann, R., Jones, K.C., 2004. Evidence for dynamic air-water coupling and cycling of persistent organic pollutants over the open Atlantic Ocean. Environ. Sci. Technol. 38, 2617–2625.
Jia, H., Li, Y.F., Wang, D., Cai, D., Yang, M., Ma, J., Hu, J., 2009. Endosulfan in China 1-gridded usage inventories. Environ. Sci. Pollut. Res. Int. 16, 295–301.
Jin, G.Z., Kim, S.M., Lee, S.Y., Park, J.S., Kim, D.H., Lee, M.J., Sim, K.T., Kang, H.G., Kim, I.G., Shin, S.K., Seok, K.S., Hwang, S.R., 2013. Levels and potential sources of atmospheric organochlorine pesticides at Korea background sites. Atmos. Environ. 68, 333–342.
Jones, K.C., de Voogt, P., 1999. Persistent organic pollutants (POPs): state of the science. Environ. Pollut. 100, 209–221.
Kallenborn, R., Oehme, M., Wynn-Williams, D.D., Schlabach, M., Harris, S., 1998. Ambient air levels and atmospheric long-range transport of persistent organochlorines to Signy Island, Antarctica. Sci. Total Environ. 220, 167–180.
Li, J., Zhang, G., Guo, L., Xu, W., Li, X., Lee, C.S.L., Ding, A., Wang, T., 2007. Organochlorine pesticides in the atmosphere of Guangzhou and Hong Kong: regional sources and long-range atmospheric transport. Atmos. Environ. 41, 3889–3903.
Li, J., Zhang, G., Qi, S.H., Li, X.D., Peng, X.Z., 2006. Concentrations, enantiomeric compositions, and sources of HCH, DDT and chlordane in soils from the Pearl River Delta, South China. Sci. Total Environ. 372, 215–224.
Li, Y.F., Cai, D.J., Singh, A., 1998. Technical hexachlorocyclohexane use trends in China and their impact on the environment. Archives Environ. Contam. Toxicol. 35, 688–697.
Li, Y.F., 1999. Global technical hexachlorocyclohexane usage and its contamination consequences in the environment: from 1948 to 1997. Sci. Total Environ. 232, 121–158.
Li, Y.F., Bidleman, T.F., 2003. Correlation between global emissions of α-hexachlorocyclohexane and its concentrations in the Arctic air. J. Environ. Informatics 1, 52–57.
Li, Y., Lin, T., Wang, F., Ji, T., Guo, Z., 2015. Seasonal variation of polybrominated diphenyl ethers in PM2.5 aerosols over the East China Sea. Chemosphere 119, 675–681.
Lin, T., Hu, L., Shi, X., Li, Y., Guo, Z., Zhang, G., 2012a. Distribution and sources of organochlorine pesticides in sediments of the coastal East China Sea. Mar. Pollut. Bull. 64, 1549–1555.
Lin, T., Li, J., Xu, Y., Liu, X., Luo, C., Cheng, H., Chen, Y., Zhang, G., 2012b. Organochlorine pesticides in seawater and the surrounding atmosphere of the marginal seas of China: spatial distribution, sources and air-water exchange. Sci. Total Environ. 435–436, 244–252.
Lin, T., Hu, Z., Zhang, G., Li, X., Xu, W., Tang, J., Li, J., 2009. Levels and mass burden of DDTs in sediments from fishing harbors: the importance of DDT-containing antifouling paint to the coastal environment of China. Environ. Sci. Technol. 43, 8033–8038.
Liu, X., Zhang, G., Li, J., Yu, L.L., Xu, Y., Li, X.D., Kobara, Y., Jones, K.C., 2009. Seasonal patterns and current sources of DDTs, chlordanes, hexachlorobenzene, and endosulfan in the atmosphere of 37 Chinese cities. Environ. Sci. Technol. 43, 1316–1321.
Lohmann, R., Gioia, R., Jones, K.C., Nizzetto, L., Temme, C., Xie, Z., Schulz-Bull, D., Hand, I., Morgan, E., Jantunen, L., 2009. Organochlorine pesticides and PAHs in the surface water and atmosphere of the North Atlantic and Arctic Ocean. Environ. Sci. Technol. 43, 5633–5639.
Ma, J., Venkatesh, S., Li, Y.F., Cao, Z., Daggupaty, S., 2005. Tracking toxaphene in the North American Great Lakes basin. 2. A strong episodic long-range transport event. Environ. Sci. Technol. 39, 8132–8141.
Ma, W.L., Sun, D.Z., Shen, W.G., Yang, M., Qi, H., Liu, L.Y., Shen, J.M., Li, Y.F., 2011. Atmospheric concentrations, sources and gas-particle partitioning of PAHs in Beijing after the 29th Olympic Games. Environ. Pollut. 159, 1794–1801.
Nizzetto, L., Macleod, M., Borgå, K., Cabrerizo, A., Dachs, J., Guardo, A.D., Ghirardello, D., Hansen, K.M., Jarvis, A., Lindroth, A., Ludwig, B., Monteith, D., Perlinger, J.A., Scheringer, M., Schwendenmann, L., Semple, K.T., Wick, L.Y., Zhang, G., Jones, K.C., 2010. Past, present, and future controls on levels of persistent organic pollutants in the global environment. Environ. Sci. Technol. 44, 6526–6531.
Oehme, M., 1991. Further evidence for long-range air transport of polychlorinated aromates and pesticides: North America and Eurasia to the Arctic. Ambio 20, 293–297.
Paasivirta, J., Sinkkonen, S., Mikkelson, P., Rantio, T., Wania, F., 1999. Estimation of vapor pressures, solubilities and Henry's law constants of selected persistent organic pollutants as functions of temperature. Chemosphere 39, 811–832.
Qiu, X., Zhu, T., Li, J., Pan, H., Li, Q., Miao, G., Gong, J., 2004. Organochlorine

pesticides in the air around the Taihu Lake, China. Environ. Sci. Technol. 38, 1368–1374.
Qiu, X., Zhu, T., Yao, B., Hu, J., Hu, S., 2005. Contribution of dicofol to the current DDT pollution in China. Environ. Sci. Technol. 39, 4385–4390.
Rodriguez-Garrido, B., Lu-Chau, T., Feijoo, G., Macias, F., Monterrroso, M., 2010. Reductive dechlorination of α-, β-, γ-, and δ-hexachlorocyclohexane isomers with hydroxocobalamin, in soil slurry systems. Environ. Sci. Technol. 44, 7063–7069.
Tao, S., Liu, W., Li, Y., Yang, Y., Zuo, Q., Li, B., Cao, J., 2008. Organochlorine pesticides contaminated surface soil as reemission source in the Haihe Plain, China. Environ. Sci. Technol. 42, 8395–8400.
Tian, C., Liu, L., Ma, J., Tang, J., Li, Y.F., 2011. Modeling redistribution of α-HCH in Chinese soil induced by environment factors. Environ. Pollut. 159, 2961–2967.
Tian, C., Ma, J., Chen, Y., Liu, L., Ma, W., Li, Y., 2012. Assessing and forecasting atmospheric outflow of α-HCH from China on intra-, inter-, and decadal time scales. Environ. Sci. Technol. 46, 2220–2227.
Wania, F., Mackay, D., 1995. A global distribution model for persistent organic chemicals. Sci. Total Environ. 160–161, 211–232.
Wania, F., Mackay, D., Li, Y.-F., Bidleman, T.F., Strand, A., 1999. Global chemical fate of α-hexachlorocyclohexane. 1. Evaluation of a global distribution model. Environ. Toxicol. Chem. 18, 1390–1399.
Wang, F., Lin, T., Li, Y., Ji, T., Ma, C., Guo, Z., 2014. Sources of polycyclic aromatic hydrocarbons in PM2.5 over the East China Sea, a downwind domain of East Asian continental outflow. Atmos. Environ. 92, 484–492.
Wang, Q., Zhao, L., Fang, X., Xu, J., Li, Y., Shi, Y., Hu, J., 2012. Gridded usage inventories of chlordane in China. Front. Environ. Sci. Eng. 7, 10–18.
Wang, T.Y., Lu, Y.L., Zhang, H., Shi, Y.J., 2005. Contamination of persistent organic pollutants (POPs) and relevant management in China. Environ. Int. 31, 813–821.
Weber, J., Halsall, C.J., Muir, D., Teixeira, C., Small, J., Solomon, K., Hermanson, M., Hung, H., Bidleman, T., 2010. Endosulfan, a global pesticide: a review of its fate in the environment and occurrence in the Arctic. Sci. Total Environ. 408, 2966–2984.
Wei, D., Kameya, T., Urano, K., 2007. Environmental management of pesticidal POPs in China: past, present and future. Environ. Int. 33, 894–902.
Wurl, O., Potter, J.R., Obbard, J.P., Durville, C., 2006. Persistent organic pollutants in the equatorial atmosphere over the open Indian Ocean. Environ. Sci. Technol. 40, 1454–1461.
Xu, K., Milliman, J.D., 2009. Seasonal variations of sediment discharge from the Yangtze River before and after impoundment of the Three Gorges Dam. Geomorphology 104, 276–283.
Xu, Y., Tian, C., Ma, J., Zhang, G., Li, Y., Ming, L., Li, J., Chen, Y., Tang, J., 2012. Assessing environmental fate of β-HCH in Asian soil and association with environmental factors. Environ. Sci. Technol. 46, 9525–9532.
Zhang, G., Li, J., Cheng, H., Li, X., Xu, W., Jones, K.C., 2007. Distribution of organochlorine pesticides in the northern South China Sea: implications for land outflow and air-sea exchange. Environ. Sci. Technol. 41, 3884–3890.
Zhang, G., Parker, A., House, A., Mai, B., Li, X., Kang, Y., Wang, Z., 2002. Sedimentary records of DDT and HCH in the Pearl River Delta, South China. Environ. Sci. Technol. 36, 3671–3677.